Journal of Ceramic Processing Research. Vol. 18, No. 4, pp. 301~304 (2017)

J O U R N A L O F
Ceramic Processing Research

Improvement of leakage and ferroelectric properties of Mn-doped $BiFeO_3$ thin films

Fengqing Zhang[a,b], Suhua Fan[c,*], Cuijuan Wang[a,b], Xiaobin Xie[a,b] and Xiaodong Guo[c]

[a]*Co-Innovation Center for Green Building of Shandong Province, Shandong Jianzhu University, Jinan 250101, China*
[b]*School of Materials Science and Engineering, Shandong Jianzhu University, Jinan 250101, China*
[c]*Shandong Women's University, Jinan 250300, China*

A series of Mn-doped $BiFeO_3$ (BFO) films were successfully deposited on the ITO/glass substrates by sol-gel method combining layer by layer annealing process. The effects of Mn content on the film texture, leakage current, conduction mechanism and ferroelectric behavior of the deposited BFO films were systematically investigated. Compared to undoped BFO thin films, all the Mn-doped films showed refined grains, defectless microstructure and improved electric properties. The conduction mechanism changed from space charge limited conduction (SCLC) to Ohmic conduction gradually as Mn content increased. Meanwhile, the Mn-doped BFO films showed remarkable asymmetrical coercive field, which was induced by the high content of defect complexes of $(V_{O^{2-}})^{\cdot\cdot}$-$(A^{2+}_{Fe^{3+}})'$.

Key words: Ferroelectrics, Sol-gel process, Thin films, X-ray diffraction.

Introduction

In recent years, perovskite-type $BiFeO_3$ (BFO) has been studied extensively due to its promising applications for data storage and microelectromechanical systems [1]. It is a lead-free multiferroic material with relatively high Curie temperature ($T_C \sim 850$ °C) and Néel temperature ($T_N \sim 370$°C) [1, 2]. In addition, BFO possesses a large polarization and a low temperature of crystallization, which is desirable for high density FeRAM.

In comparison with bulk ceramic BFO, BFO thin films exhibit rather different electrical behavior, for example, a much larger polarization [3-5]. In addition, BFO thin films can be much smaller and more versatile when made into functional devices, which will promote the miniaturization and integration of the microelectronic devices. However, utilization of BFO thin films for devices is still challenging due to the large leakage current density and poor fight-against-wear property resulted from Bi volatility and valance fluctuation of Fe^{3+} [6]. Up to now, the most effective way to solve these problems is proved to be doping modification. For example, heterovalent Ti, Mn, Zn, W and Nb atoms on B (Fe-) site have been extensively used to replace Fe atoms to suppress the valence fluctuation of Fe^{3+} and reduce the leakage current density [7-9]. Among them, the substitution of Mn atom has been reported to reveal its role in improving the properties of BFO thin films. However, limited reports about the change of conduction mechanism with increasing Mn doping content are available [10-11].

In this work, Mn has been substituted for Fe-site to improve the microstructure and electrical properties of BFO thin films. A series of $BiFe_{1-x}Mn_xO_3$ (BFMO. x = 0, 0.015, 0.03, 0.045, 0.06) thin films have been deposited on ITO/glass substrates by sol-gel method combining layer by layer annealing process. The effect of Mn doping content on the microstructure, leakage current density and ferroelectric properties of BFO thin films has been studied systematically. In addition, the conduction mechanism in BFMO thin films is also discussed.

Experimental

The BFMO thin films were prepared by sol-gel process. The BFMO precursor solution was synthesized by dissolving bismuth nitrate pentahydrate, iron nitrate enneahydrateand manganese acetate tetrahydrateinto ethylene glycol and acetic acid by stirring for 8hrs at room temperature, and then a moderate amount of acetylacetone was added as chelating agent. 10% excess Bi was used to compensate the possible volatility of Bi. The as-prepared solution was deposited on ITO/glass substrates by spin coating at 4000 rpm for 30 sec. Then, each layer was dried on the hot plate at 250 °C for 180 sec to accelerate the volatilization of the organic compounds. The dried films was pyrolyzed at 350 °C for 180sec and annealed at 500 °C for 300 sec. The coating and annealing process were repeated until the required thickness was obtained.

The structure and orientation of the crystallined films was characterized by Bruker D8 diffractometer in θ-2θ

*Corresponding author:
Tel : +86 531 86526688
Fax: +86 531 86526786
E-mail: suhuafan@126.com.

mode with Cu Kα rediation. The surface morphology of the films was was detected by a scanning electron microscopy (SEM, FEI Nova NanoSEM 450). The ferroelectric and leakage properties were investigated by a ferroelectric tester (Radiant Multiferroic). In order to investigate the electrical properties of the films, an ion sputtering equipment was employed to deposit Au top electrodes with a diameter of 500 μm through a shadow mask. In order to simplify description, the BFMO thin films with Mn content of 0%, 1.5%, 3%, 4.5% and 6% is denoted as BFM0, BFM1.5, BFM3, BFM4.5 and BFM6, respectively.

Results and Discussions

Fig. 1 shows the XRD patterns of BFMO films with different Mn doping content in the range of 2θ from 20 ° to 60 °. The diffraction peaks are indexed with ICDD Card No. 86-1518. Evidently, all BFMO films grown on ITO/glass substrates are well crystallized, and no reflections that would be indicative of second phases are detected. This can be attributed to the stable precursor solutions and appropriate heat treatment process. It is worth noting that the strongest diffraction peak change from (012) to (104)/(110) peak, which indicates the change in growth mode and preferential growth of (104)/(110) with Mn doping.

In order to clearly understand the evolution of structure as Mn content increases, the average grain size was calculated by Scherrer's equation and plotted in the inset of Fig. 1. As shown in the inset, compared with pure BFO thin films, the average grain size decreases obviously in all Mn-doped films, which indicates the grain refining effect of Mn substitution. This can be largely attributed to the decrease of crystallinity after Mn doping. However, as Mn content increases from 1.5% to 6%, the grainsize increases gradually, though still smaller than that of the pure phase. The small change could be attributed to the small difference in ionic radii of dopant.

SEM images showing the surface microstructures of Mn-doped films are presented in Fig. 2. All the samples are well-crystallized. The undoped BFO films shows porous microstructure, which could impair the properties of the films severely. The defective microstructure can lead to the increase in leakage directly by forming leakage tunnels. By contrast, Mn-substitution was found to be effective in improving the microstructure of BFO films, for all Mn-doped BFO thin films showed dense, uniform and crack-free microstructure. The homogeneous and defectless microstructure may affect the ferroelectric properties, which would be discussed later.

Leakage current density *vs* electric field (*J-E*) curves of Mn-doped thin films are plotted in Fig. 3. The undoped BFO films possessed a slightly lower leakage current in the low electric field region. However, with the increase of electric field, the current density of the

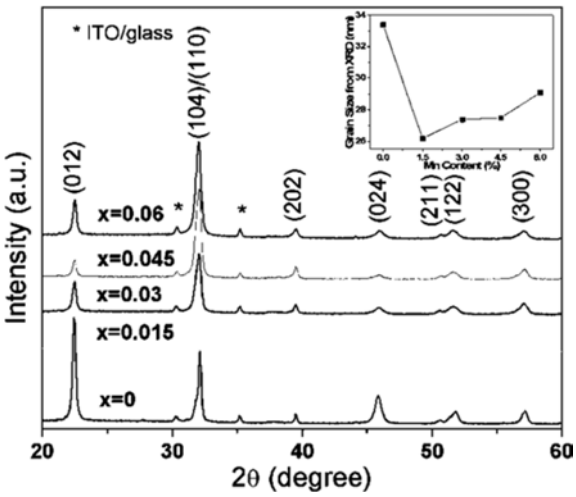

Fig. 1. XRD patterns of $BFMO_x$ (x = 0, 0.015, 0.03, 0.045, 0.06) thin films.

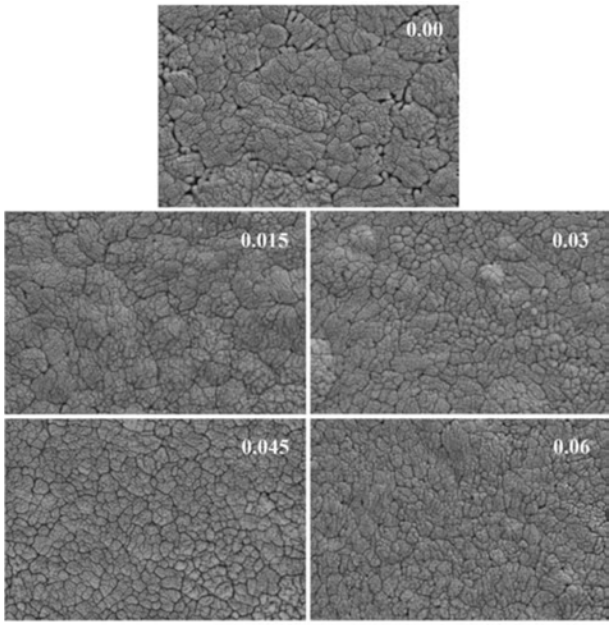

Fig. 2. SEM images of $BFMO_x$ (x = 0, 0.015, 0.03, 0.045, 0.06) thin films.

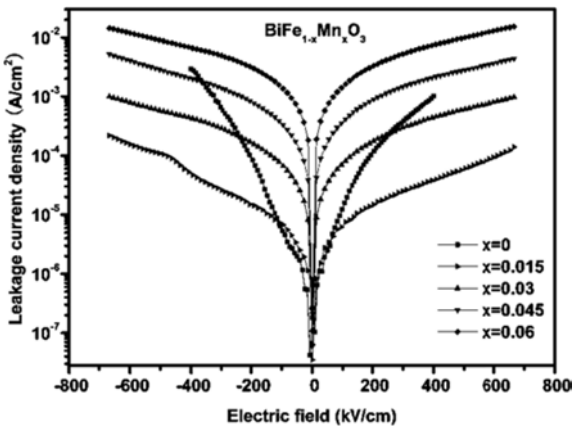

Fig. 3. J-E curves of $BFMO_x$ (x=0, 0.015, 0.03, 0.045, 0.06) thin films.

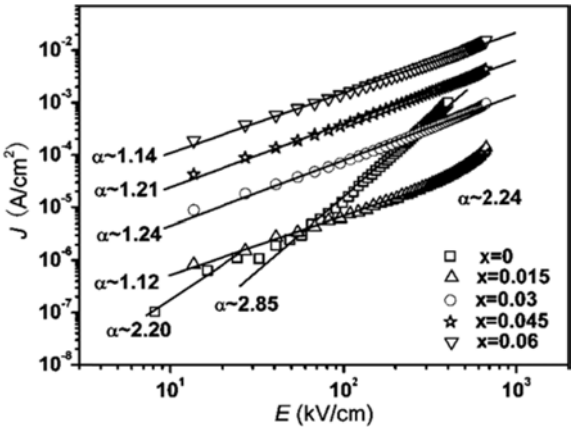

Fig. 4. *J-E* curves of $BFMO_x$ (x = 0, 0.015, 0.03, 0.045, 0.06) thin films in logarithmic plots.

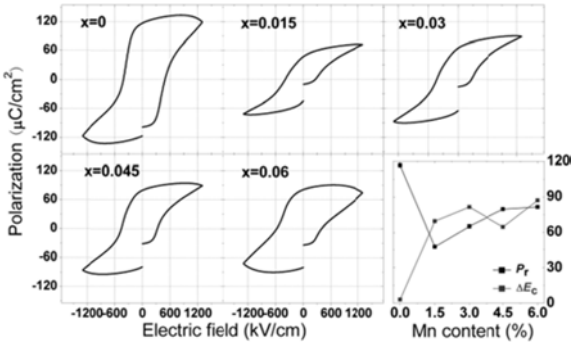

Fig. 5. *P-E* hysteresis loops of $BFMO_x$ (x = 0, 0.015, 0.03, 0.045, 0.06) thin films.

undoped BFO films increases linearly, and the films undergo a breakdown when the electric field was above 400 kV/cm. This is mainly due to the high defects density in the films. Merely 1.5% Mn-substitution is proved to be quite effective in reduce the leakage current density of BFO films and improve the anti-breakdown properties. Meanwhile, the leakage current density of the Mn-doped films tended to be stable when the electric field was above 200 kV/cm. Interestingly, the current density increased gradually as the Mn content increases. As shown from the inset of Fig. 1, the grains grow larger as Mn content increases, the amount of grain boundaries, hence, tended to decrease with it. As a result, the obstruction of grain boundaries on current weakens, which lead to the increase in leakage current density.

Fig. 4 shows the logarithmic plots of dependence of *J* as a function of *E* for various Mn-doped BFO thin films. The plots reveals a near linearity in the range of applied electric fields investigated and they obey the power law of $J \propto E^{\alpha}$. The undoped BFO thin films was found to be subjected to SCLC mechanism with the fitting exponentials of $\alpha \sim 2.20$ and 2.85. The α value of BFM1.5 in the low field region is around 1, suggesting that thermally stimulated Ohmic conduction dominates. With increase in the electric field, electrons are injected into the films, and the current becomes larger than that of thermally stimulated electrons. In the high field region, the α value is approximately 2, which agrees well with the SCLC mechanism. The conduction mechanism of BFM3, BFM4.5 and BFM6 was found to be only subjected to Ohmic mechanism with the α values of 1.24, 1.21 and 1.14, respectively, and the precision for Ohmic mechanism was also improved with Mn content. Briefly, with Mn content increases from 0% to 6%, the leakage mechanism undergoes a transition from an SCLC conduction to the Ohmic conduction.

The *P-E* ferroelectric hysteresis loops of BFMO films measured at 200Hz are shown in fig. 5. To clearly characterize the ferroelectric properties, we also plotted the remnant polarization (P_r) and coercive field (ΔE_c) of BFMO films as a function of Mn doping content, as shown in the inset of Fig. 5. As shown in the figure, all films exhibit well-defined loops. The pure BFO films exhibit a rounded loop, indicting the contribution from leakage current. This can be attributed to the high defects density resulted from oxygen vacancies and valence fluctuation. A small amount of Mn substitution is proved to be effective in suppressing the leakage current in BFO films. However, all Mn-doped films show smaller P_r value and asymmetric coercivefield, which can be induced by the higher content of defect complexes of $(V_{O^{2-}})^{\cdot\cdot}$-$(A^{2+}_{Fe^{3+}})'$. The defect complexes can align along the direction of spontaneous polarization, thus domains exhibit a tendency to stabilize in one polarization state over another. This is known as the process of aging, which has been extensively detected in other ferroelectric materials such as $Pb(Zr,Ti)O_3$, $Bi_4Ti_3O_{12}$, $SrBi_2Ta_2O_9$, and $BaTiO_3$ [12-15]. A slightly larger remnant polarization and better rectangularity are observed as Mn content increased. At the same time, the BFO films with Mn content of 6% show similar leakage characteristics as undoped ones, indicating a severe leakage current. The phenomenon agrees well with the leakage behaviors shown in Fig. 3.

Conclusions

The undoped and Mn-doped BFO thin films were prepared by sol-gel method on the ITO/glass substrates. Compared to undoped BFO thin films, all the Mn-doped films showed refined grains, defectless microstructure and improved electric properties. The conduction mechanism of undoped BFO thin films was found to be SCLC, and that of Mn-doped BFO thin films was dominated by Ohmic conduction. However, the Mn-doped BFO films were found to show remarkable asymmetrical coercive field, which was induced by the aging behavior in these thin films.

Acknowledgments

This work was supported by funding from A Project of Shandong Province Higher Educational Science and Technology Program (Grant No. J15LA05), the National Natural Science Foundation of China (Grant Nos.51272142) and Research Fund for the Doctoral Program of Shandong Jianzhu University (Grant Nos. XNBS1626).

References

1. N.A. Spaldin, S.W. Cheong, and R.Ramesh, Multiferroics: Past, present, and future, Phys. Today 63[10] (2010) 38-43.
2. J. Wang, J.B. Neaton, H. Zheng, V. Nagarajan, S.B. Ogale, B. Liu, D. Viehland, V. Vaithyanathan, D.G. Schlom, U.V. Waghmare, N.A. Spaldin, K.M. Rabe, M. Wuttig, R. Ramesh, Science .299 (2003)1719-1722.
3. A.R. Akbashev, G.N. Chen, J.E. Spanier, Nano Lett. 14 (2014) 44-49.
4. G.H. Dong, G.Q. Tan, W.L. Liu, A. Xia , H.J. Ren, Ceram. Int. 40 (2014) 1919-1925.
5. J.S. Park, Y.J. Yoo, J.S. Hwang, J.H. Kang, B.W. Lee, Y.P. Lee, J. Appl. Phys. 115 (2014) 013904-1-5.
6. P. Uniyal, K.L. Yadav, J. Phys.: Condens Matter. 21 (2009) 012205-012210.
7. L. Cheng, G.D. Hu, B. Jiang, C.H. Yang, W.B. Wu, and S.H. Fan, Appl. Phys. Express 3[10] (2010) 101501-101504.
8. J.M. Park, F. Gotoda, S. Nakashima, T. Kanashima, and M. Okuyama, Curr. Appl. Phys. 11 (2011) S270-273.
9. T. Kawae, Y. Terauchi, H. Tsuda, M. Kumeda, and A. Morimoto, Appl. Phys. Lett. 94 (2009) 112904-112908.
10. A. Lahmar, S. Habouti, M. Dietze, C.H. Solterbeck, and M. Es-Souni , Appl. Phys. Lett. 94 (2009) 012903-012907.
11. V.R. Reddy, D. Kothari, A. Gupta, and S.M. Gupta, Appl. Phys. Lett. 94 (2015) 082505-082508.
12. E. Ramos-Moorea, D. Ledermanb, A.L. Cabreraa, Appl. Surf. Sci. 258[3] (2013) 1181-1183.
13. N. Tohge, Y. Fukuda, and T. Minami, J. Appl. Phys. 31 [12] (1992) 4016-4017.
14. Y. Ding, J.S. Liu, I. Maclaren, Y.N. Wang, and K.H. Kuo, Ferroelectr. 261[1] (2001) 37-46.
15. X. Zhao, W. Chen, L. Zhang, and L. Zhong, J. Alloys Compd. 618 (2015) 707-711.